Journal of Statistical Mechanics: Theory and Experiment
An IOP and SISSA journal

PAPER: Classical statistical mechanics, equilibrium and non-equilibrium

The Enskog–Vlasov equation: a kinetic model describing gas, liquid, and solid

E S Benilov[1] **and M S Benilov**[2,3]

[1] Department of Mathematics and Statistics, University of Limerick, V94 T9PX, Ireland
[2] Departamento de Física, CCCEE, Universidade da Madeira, Largo do Município, 9000 Funchal, Portugal
[3] Instituto de Plasmas e Fusão Nuclear, Instituto Superior Técnico, Universidade de Lisboa, Lisboa, Portugal
E-mail: Eugene.Benilov@ul.ie and benilov@uma.pt

Received 15 April 2019
Accepted for publication 10 August 2019
Published 22 October 2019

Online at stacks.iop.org/JSTAT/2019/103205
https://doi.org/10.1088/1742-5468/ab3ccf

Abstract. The Enskog–Vlasov (EV) equation is a semi-empiric kinetic model describing gas–liquid phase transitions. In the framework of the EV equation, these correspond to an instability with respect to infinitely long perturbations, developing in a gas state when the temperature drops below (or density rises above) a certain threshold. In this paper, we show that the EV equation describes one more instability, with respect to perturbations with a finite wavelength and occurring at a higher density. This instability corresponds to fluid-solid phase transition and the perturbations' wavelength is essentially the characteristic scale of the emerging crystal structure. Thus, even though the EV model does not describe the fundamental physics of the solid state, it can 'mimic' it—and, thus, be used in applications involving both evaporation and solidification of liquids. Our results also predict to which extent a pure fluid can be overcooled before it definitely turns into a solid.

Keywords: classical phase transitions, kinetic theory of gases and liquids

J. Stat. Mech. (2019) 103205

1742-5468/19/103205+14$33.00

Contents

1. Introduction **2**

2. The Enskog–Vlasov model **3**
2.1. The EV equation 3
2.2. Steady solutions of the EV equation 6

3. The stability analysis **6**

4. The results **8**

5. Discussion **10**

6. Concluding remarks **13**
Acknowledgments **13**

References **13**

1. Introduction

The Enskog–Vlasov (EV) kinetic equation comprises the Enskog collision integral for dense fluids [1] and a Vlasov term describing the van-der-Waals force. The first version of the EV equation [2] was based on the original form of the Enskog integral—which, as shown in [3], does not comply with the Onsager relations. [4] proposed a modification of the Enskog integral free from this shortcoming, which was incorporated in the EV model in [5, 6]. Grmela and Garcia-Colin [7] showed that an H-theorem holds for the EV equation only subject to a certain restriction of its coefficients, and [8] proposed a version of the EV equation that satisfies this restriction and conserves energy as well (all of the previous versions do not).

Note that, in kinetic models, phase transitions correspond to instabilities. For the original version of the EV equation, the presence of an instability has been shown in [9], and it was interpreted as gas–liquid phase transition.

In the present paper, we report the results of a more detailed study. Using the EV equation that conserves energy and satisfies an H-theorem, we find *two* instabilities, with respect to infinite- and finite-wavelength perturbations—interpreted as gas–liquid and fluid-solid transitions, respectively. The latter result comes as a surprise, as the EV equation was conceived as a tool for modeling of fluids only. We show, however, that it admits periodic solutions capable of 'mimicking' the solid phase.

The present paper has the following structure. In section 2, we introduce the Enskog–Vlasov equation and, in section 3, carry out the stability analysis of its spatially homogeneous solutions. The general results are illustrated by applying them to noble gases in sections 4 and 5.

J. Stat. Mech. (2019) 103205

2. The Enskog–Vlasov model

2.1. The EV equation

Consider a fluid of hard spheres of diameter D, characterized by the one-particle distribution function $f(\mathbf{r}, \mathbf{v}, t)$ where $\mathbf{r}$ is the position vector, $\mathbf{v}$ the velocity, and t the time.

Let the molecules exert on each other a force with a pair-wise potential $\Phi(r)$, modeling physically the van der Waals interaction of molecules. Let $\Phi(r)$ be a monotonically growing function of r, so that the van der Waals force is attractive at all distances. Letting also, without loss of generality, $\Phi \to 0$ as $r \to \infty$, we can assume that $\Phi(r) < 0$ for all r.

As seen later, the main characteristic of Φ—one that affects the fluid's macroscopic properties—is

$$E = -\int \Phi(r)\, \mathrm{d}^3\mathbf{r}. \tag{1}$$

Using E, D, the molecular mass m, and the Boltzmann constant k_B, we introduce the following nondimensional variables:

$$\mathbf{r}_\mathrm{nd} = \frac{\mathbf{r}}{D}, \qquad \mathbf{v}_\mathrm{nd} = \left(\frac{m}{ED^3}\right)^{1/2} \mathbf{v}, \qquad t_\mathrm{nd} = \left(\frac{ED}{m}\right)^{1/2} t,$$

$$f_\mathrm{nd} = \frac{k_\mathrm{B} E^{1/2} D^{3/2}}{m^{3/2}} f, \qquad \Phi_\mathrm{nd} = \frac{\Phi}{ED^3}.$$

Note that, due to (1), the nondimensional potential Φ_nd satisfies (the subscript $_\mathrm{nd}$ omitted)

$$\int \Phi(r)\, \mathrm{d}^3\mathbf{r} = -1. \tag{2}$$

In terms of the nondimensional variables, the Enskog–Vlasov equation has the form ($_\mathrm{nd}$ omitted)

$$\begin{aligned} \frac{\partial f(\mathbf{r}, \mathbf{v}, t)}{\partial t} + \mathbf{v} \cdot \boldsymbol{\nabla} f(\mathbf{r}, \mathbf{v}, t) + \mathbf{F}(\mathbf{r}, t) \cdot \frac{\partial f(\mathbf{r}, \mathbf{v}, t)}{\partial \mathbf{v}} \\ = \int\int \left[\eta(\mathbf{r}, \mathbf{r} + \boldsymbol{\kappa}, t)\, f(\mathbf{r}, \mathbf{v}', t)\, f(\mathbf{r} + \boldsymbol{\kappa}, \mathbf{v}_1', t)\right. \\ \left. - \eta(\mathbf{r}, \mathbf{r} - \boldsymbol{\kappa}, t)\, f(\mathbf{r}, \mathbf{v}, t)\, f(\mathbf{r} - \boldsymbol{\kappa}, \mathbf{v}_1, t)\right] \mathbf{g} \cdot \boldsymbol{\kappa}\, \mathrm{H}(\mathbf{g} \cdot \boldsymbol{\kappa})\, \mathrm{d}^2\boldsymbol{\kappa}\, \mathrm{d}^3\mathbf{v}_1, \end{aligned} \tag{3}$$

where H is the Heaviside function,

$$\mathbf{F}(\mathbf{r}, t) = -\boldsymbol{\nabla} \int n(\mathbf{r}_1, t)\, \Phi(|\mathbf{r} - \mathbf{r}_1|)\, \mathrm{d}^3\mathbf{r}_1 \tag{4}$$

is the collective van der Waals force,

$$n(\mathbf{r}, t) = \int f(\mathbf{r}, \mathbf{v}, t)\, \mathrm{d}^3\mathbf{v} \tag{5}$$

J. Stat. Mech. (2019) 103205

is the number density, $\boldsymbol{\kappa}$ is a unit vector parameterizing all possible orientations of a pair of spheres (molecules) at the moment of collision, and the post-collision velocities $(\mathbf{v}', \mathbf{v}_1')$ are related to the pre-collision ones, $(\mathbf{v}, \mathbf{v}_1)$, by

$$\mathbf{v}' = \mathbf{v} + \boldsymbol{\kappa}\,(\mathbf{g}\cdot\boldsymbol{\kappa})\,, \qquad \mathbf{v}_1' = \mathbf{v}_1 - \boldsymbol{\kappa}\,(\mathbf{g}\cdot\boldsymbol{\kappa})\,, \qquad \mathbf{g} = \mathbf{v}_1 - \mathbf{v}. \tag{6}$$

The coefficient $\eta(\mathbf{r}, \mathbf{r}_1, t)$ which appears in the collision integral is, generally, a functional of $n(\mathbf{r}, t)$. It originates from the main assumption of the EV theory that the two-particle distribution function $f^{(2)}(\mathbf{r}, \mathbf{v}, \mathbf{r}_1, \mathbf{v}_1, t)$ is related to the singlet $f(\mathbf{r}, \mathbf{v}, t)$ by

$$f^{(2)}(\mathbf{r}, \mathbf{v}, \mathbf{r}_1, \mathbf{v}_1, t) = \eta(\mathbf{r}, \mathbf{r}_1, t)\, f(\mathbf{r}, \mathbf{v}, t)\, f(\mathbf{r}_1, \mathbf{v}_1, t).$$

Given a specific expressions for η, equations (3)–(6) fully determine the evolution of f.

There are three approaches to choosing $\eta(\mathbf{r}, \mathbf{r}_1, t)$:

(i) In the original Enskog theory [1], η is a function of the number density evaluated at the midpoint between the colliding molecules, i.e. $n(\frac{1}{2}(\mathbf{r} + \mathbf{r}_1), t)$. This function is supposed to be such that the EV model describes the equation of state (EoS) of the fluid under consideration with the best possible accuracy.

(ii) The authors of [4] derived η from a hypothesis that the n-particle distribution function is represented by a product of singlet distributions and (sic!) a factor excluding all states where the hard spheres overlap. This hypothesis does hold at equilibrium, but should be considered as approximate otherwise. Another difficulty associated with this approach is that the resulting η is defined through a limiting procedure involving multiple integrals of increasing order, making it impossible to solve the EV equation numerically.

(iii) The authors of [8] assumed

$$\eta(\mathbf{r}, \mathbf{r}_1, t) = 1 + \sum_{l=2}^{L} c_l \int^l \left[\prod_{i=2}^{l} n(\mathbf{r}_i, t)\, \mathrm{H}(1 - |\mathbf{r} - \mathbf{r}_i|)\, \mathrm{H}(1 - |\mathbf{r}_1 - \mathbf{r}_i|)\right] \times \left[\prod_{i=2}^{l-1} \prod_{j=i+1}^{l} \mathrm{H}(1 - |\mathbf{r}_i - \mathbf{r}_j|)\right] \prod_{i=1}^{l} \mathrm{d}^3\mathbf{r}_i, \tag{7}$$

where $\int^l$ denotes l repeated integrals, and the coefficients c_2, c_3, $c_4 \ldots c_L$ are to be chosen to fit the properties of the fluid under consideration. Note that the 'proper' hard-sphere η derived in [4] is a particular case of (7)—one with $L = \infty$ and certain values of c_l (which are not easy to calculate).

It turns out that the choice of η affects the fundamental properties of the EV equation.

Consider, for example, the entropy of the system, which is traditionally assumed [2, 7, 10, 11] to have the form

$$S = -\int\int f(\mathbf{r}, \mathbf{v}, t) \ln f(\mathbf{r}, \mathbf{v}, t)\, \mathrm{d}^3\mathbf{v}\, \mathrm{d}^3\mathbf{r} + Q[n],$$

J. Stat. Mech. (2019) 103205

where the non-ideal contribution $Q[n]$ is a functional depending on $n(\mathbf{r},t)$[4]. Then, the H-theorem holds if and only if $Q[n]$ and η are inter-related by

$$\boldsymbol{\nabla}\frac{\delta Q[n]}{\delta n(\mathbf{r},t)} = -\int \eta(\mathbf{r},\mathbf{r}_1,t)\, n(\mathbf{r}_1,t)\,(\mathbf{r}_1-\mathbf{r})\,\delta(|\mathbf{r}-\mathbf{r}_1|-1)\,\mathrm{d}^3\mathbf{r}_1 \tag{8}$$

(see [7] and, for more detail, appendix A of [8]). The question of existence of $Q[n]$ as a solution of equation (8) for a given η is not trivial. If, for example, η is a function of $n\left(\frac{1}{2}(\mathbf{r}+\mathbf{r}_1),t\right)$—as in the original Enskog's theory—(8) does not seem to have a solution ~~of~~, Q. For the versions of η suggested in [4, 8], on the other hand, it does. In the latter case, an explicit expression for Q can be found,

$$\begin{aligned} Q[n] = &-\frac{1}{2}\int\int n(\mathbf{r})\, n(\mathbf{r}_1)\,\mathrm{H}(1-|\mathbf{r}-\mathbf{r}_1|)\,\mathrm{d}^3\mathbf{r}\,\mathrm{d}^3\mathbf{r}_1 \\ &-\sum_{l=2}^{L}\frac{c_l}{l\,(l+1)}\int^l\int n(\mathbf{r})\left[\prod_{i=1}^{l} n(\mathbf{r}_i)\,\mathrm{H}(1-|\mathbf{r}-\mathbf{r}_i|)\right] \\ &\times\left[\prod_{i=1}^{l-1}\prod_{j=i+1}^{l}\mathrm{H}(1-|\mathbf{r}_i-\mathbf{r}_j|)\right]\mathrm{d}^3\mathbf{r}\prod_{i=1}^{l}\mathrm{d}^3\mathbf{r}_i, \end{aligned} \tag{9}$$

where the coefficients c_l are the same as in expression (7) for η.

In this paper, we shall use η and Q given by (7) and (9), respectively.

We shall also need the function $\Theta(n)$ related to the functional $Q[n]$ by

$$\Theta(n) = -\frac{1}{n}\left(Q[n]\right)_{n=\text{const}},$$

so that (9) yields

$$\Theta(n) = \frac{2\pi}{3}n + \sum_{l=2}^{L}\frac{c_l A_l}{l\,(l+1)}n^l, \tag{10}$$

where

$$A_l = \int^l\left[\prod_{i=1}^{l}\mathrm{H}(1-|\mathbf{r}_i|)\right]\left[\prod_{i=1}^{l-1}\prod_{j=i+1}^{l}\mathrm{H}(1-|\mathbf{r}_i-\mathbf{r}_j|)\right]\prod_{i=1}^{l}\mathrm{d}^3\mathbf{r}_i \tag{11}$$

are numeric constants.

$\Theta(n)$ plays an important role in the thermodynamics of EV fluids: in particular, their EoS is [8]

$$p = nT\left[1+n\Theta'(n)\right] - \frac{1}{2}n^2 \tag{12}$$

where $\Theta' = \mathrm{d}\Theta/\mathrm{d}n$.

[4] The fact that Q depends only on n and not on f reflects the hard-sphere nature of the EV model.

J. Stat. Mech. (2019) 103205

2.2. Steady solutions of the EV equation

Physically, steady (time independent) solutions of the EV equation must have spatially uniform temperature and zero fluxes of mass, momentum, and energy—which means that they must be equilibrium states.

To find these, observe that the scattering cross-section in the Enskog integral does not depend on $\mathbf{v}$—as a result, the EV equation is consistent with the following ansatz:

$$f(\mathbf{r},\mathbf{v},t)=\frac{n(\mathbf{r})}{(2\pi T)^{3/2}}\exp\left(-\frac{|\mathbf{v}|^2}{2T}\right),$$

where T is the temperature. Substituting this ansatz into the EV equation and carrying out straightforward algebra (see [9]), we obtain the following equation for $n(\mathbf{r})$:

$$\boldsymbol{\nabla}\left[\ln n(\mathbf{r})+\frac{1}{T}\int n(\mathbf{r}_1)\,\Phi(|\mathbf{r}-\mathbf{r}_1|\,)\,\mathrm{d}^3\mathbf{r}_1\right] \tag{13}$$

$$+\int \eta(\mathbf{r},\mathbf{r}_1)\,n(\mathbf{r}_1)\,(\mathbf{r}_1-\mathbf{r})\,\delta(|\mathbf{r}_1-\mathbf{r}|-1)\,\mathrm{d}^3\mathbf{r}_1=0. \tag{14}$$

Subject to (8), this equation can be integrated,

$$\ln n(\mathbf{r})+\frac{1}{T}\int n(\mathbf{r}_1)\,\Phi(|\mathbf{r}-\mathbf{r}_1|\,)\,\mathrm{d}^3\mathbf{r}_1-\frac{\delta Q[n]}{\delta n(\mathbf{r})}=\text{const}. \tag{15}$$

This equation coincides with the Euler equation from density functional theory and also arises in equilibrium statistical mechanics (grand ensemble), where the term involving Φ is the functional derivative of the mean field contribution to the free energy, the const is the nondimensional chemical potential divided by T, and $Q[n]$ is the excess free energy. The present derivation shows that $Q[n]$ can also be interpreted as the excess contribution to, or non-ideal part of, the entropy.

3. The stability analysis

Consider the spatially uniform Maxwellian distribution $f_{\mathrm{M}}(\mathbf{v})$. To examine its stability within the framework of the EV equation, one should let

$$f(\mathbf{r},\mathbf{v},t)=f_{\mathrm{M}}(\mathbf{v})+\tilde{f}(\mathbf{r},\mathbf{v},t),$$

where $\tilde{f}(\mathbf{r},\mathbf{v},t)$ is a small perturbation. It is usually sufficient to examine harmonic perturbations only,

$$\tilde{f}(\mathbf{r},\mathbf{v},t)=\hat{f}(\mathbf{v})\,\mathrm{e}^{\mathrm{i}kz+\lambda t}, \tag{16}$$

where k is the perturbation's wavenumber, λ is its growth/decay rate, and z is one of the spatial coordinates. Substituting (16) into the linearized EV equation, one obtains an eigenvalue problem, where $\hat{f}(\mathbf{v})$ is the eigenfunction and λ the eigenvalue. If, for some k, an eigenvalue exists such that $\mathrm{Re}\lambda>0$, the base state is unstable.

J. Stat. Mech. (2019) 103205

Unfortunately, the outlined procedure implies solving a two-dimensional integral equation involving the z and normal-to-z components of $\mathbf{v}$. This equation cannot be solved analytically, and it is even difficult to be solved numerically.

Instead, we shall only examine 'frozen waves', i.e. perturbations with zero growth/decay rate, $\lambda = 0$. They are excellent stability indicators: if a frozen wave with a wavenumber k exists for a certain state, either a small increase or a small decrease of k should make it unstable. Thus, the parameter values for which the first frozen wave bifurcates from the base state corresponds to the onset of instability.

Admittedly, if $\mathrm{Re}\lambda$ changes sign while $\mathrm{Im}\lambda \neq 0$, this approach fails to detect destabilization—but in similar kinetic equations examined for stability so far [12, 13], this kind of destabilization does not occur. In the worst-case scenario, one finds some, albeit not all, of the unstable states.

Most importantly, frozen waves in the problem at hand can be found analytically—which is incomparably simpler than dealing with the general perturbations (16). For the same reason, this kind of stability analysis is often used in fluid mechanics, in particular, for liquid bridges (for example, [14, 15]).

Since frozen waves are steady, we can search for them using the steady-state reduction (15) of the full EV equation. To do so, let

$$n(\mathbf{r}) = \bar{n} + \tilde{n}(\mathbf{r}),$$

where $\bar{n}$ is the density of the base state and $\tilde{n}(\mathbf{r})$ is a perturbation. Substituting expression (10) for $Q[n]$ into equation (15), linearizing it, and letting $\tilde{n}(\mathbf{r}) = \mathrm{e}^{\mathrm{i}kz}$, we obtain an equation inter-relating k, T, and $\bar{n}$—which can be written in the form (overbars omitted)

$$T = -\frac{n\,\hat{\Phi}(k)}{1 + nF_1(k) + \sum_{l=2}^{L} c_l n^l F_l(k)}, \tag{17}$$

where

$$F_l(k) = \int^l \left[\prod_{j=1}^{l} \mathrm{H}(1 - |\mathbf{r}_j|)\right] \left[\prod_{j=1}^{l-1}\prod_{i=j+1}^{l} \mathrm{H}(1 - |\mathbf{r}_j - \mathbf{r}_i|)\right] \cos kz_l \prod_{j=1}^{l} \mathrm{d}^3\mathbf{r}_j, \tag{18}$$

and

$$\hat{\Phi}(k) = \int \Phi(r) \cos kz \, \mathrm{d}^3\mathbf{r}.$$

Note that, due to constraint (2),

$$\hat{\Phi}(0) = -1. \tag{19}$$

Functions $F_l(k)$ do not involve any parameters. The first two can be calculated analytically, and another three have been computed using the Monte-Carlo method. All five are depicted in figure 1.

Equality (17) is, essentially, an instability criterion: if a value of k exists such that (17) is satisfied for a state (n, T), this state is unstable.

J. Stat. Mech. (2019) 103205

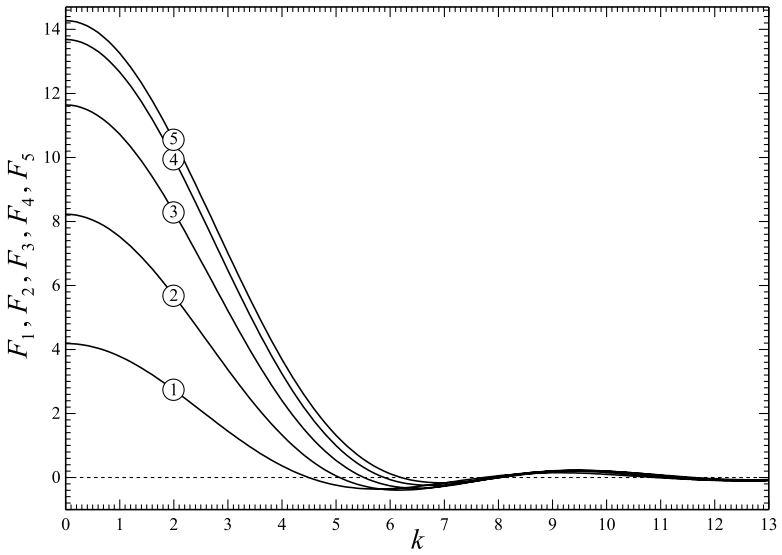

Figure 1. The functions $F_l(k)$ defined by (18). The curves are marked with the corresponding value of l.

4. The results

In what follows, we shall illustrate criterion (17) using the values for the coefficients c_l, obtained in [16] for noble gases. The series representing Q was truncated at $L = 5$, and

$$c_2 = -1.3207, \qquad c_3 = 9.9308, \tag{20}$$

$$c_4 = -18.7526, \qquad c_5 = 13.1406. \tag{21}$$

As seen later, the shape of the Vlasov potential is of little importance, so we assume, on a more or less ad hoc basis,

$$\hat{\Phi}(k) = -\frac{1}{1 + (Rk)^4}, \tag{22}$$

where R is, physically, the ratio of the spatial scale of the van der Waals force to the molecule's size. Evidently, expression (22) complies with restriction (19).

The stability criterion (17), (20)–(22) describes a one-parameter family of curves $T = T(n)$ with k being the parameter. The behavior of these curves depends on whether or not the fifth-order polynomial in n in the denominator of (17) has positive roots. Computations show that no more than one such root exists, and it (dis)appear only if $F_5(k)$ changes sign—which it does do for infinite sequence of values of k tending to infinity (see figure 1). Denoting these values by k_1, k_2, k_3..., we have computed

$$k_1 \approx 6.2042, \qquad k_2 \approx 8.0354, \qquad k_3 \approx 11.6014.$$

A straightforward analysis of expression (17) shows that, in the range

$$0 < k < k_1, \tag{23}$$

the denominator of expression (17) does *not* have positive roots. As a result—and due to quick decay of $\hat{\Phi}(k)$ as k increases—the curves $T(n)$ 'recede' within range (23)—see

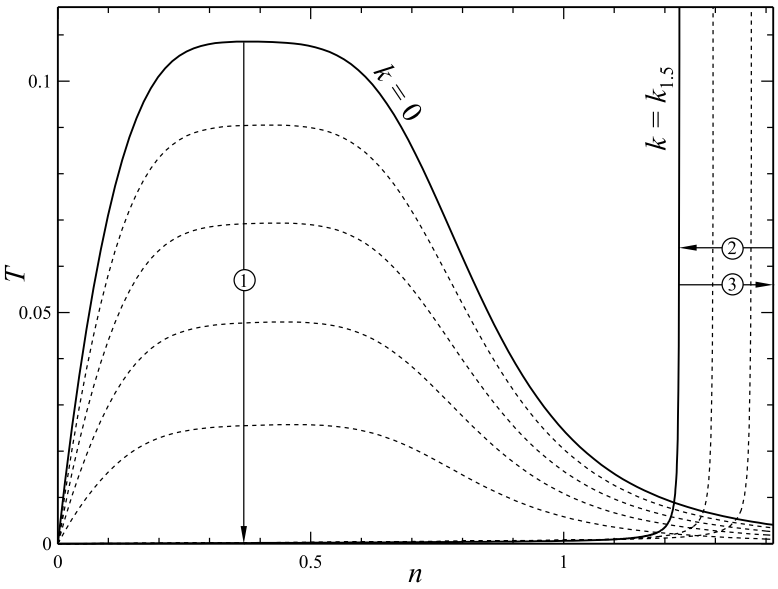

Figure 2. Existence of frozen waves on the (n, T) plane. The curves $T(n)$ are determined by (17), (20)–(22) with $R = 1$. Dotted curves within ranges (1)–(3) correspond to k being within ranges (23)–(25), respectively. The boundaries of the instability regions are shown by solid lines.

figure 2. Thus, the curve with $k = 0$ determines the boundary of an instability region, which will be referred to as IR1.

Another instability region (IR2) arises for the range $k_1 < k < k_2$—which can be conveniently subdivided into two subranges,

$$k_1 < k < k_{1.5}, \tag{24}$$

with $k_{1.5} \approx 7.129$, and

$$k_{1.5} < k < k_2. \tag{25}$$

As k changes from k_1 to $k_{1.5}$, the (real positive) root n_0 of the denominator of (17) 'travels' from $+\infty$ to $n_0 \approx 1.230$. Then, when k changes from $k_{1.5}$ to k_2, n_0 travels back to $+\infty$—i.e. the boundary of IR2 corresponds to $k = k_{1.5}$. The corresponding curve $T(n)$ is shown in figure 2 together with examples of curves for k from ranges (24) and (25).

A basic analysis of expression (17) and computations show that the instability regions corresponding to (k_2, k_3), (k_3, k_4), etc are all *inside* IR1 and IR2 and, thus, are physically unimportant.

Finally, if $n \ll 1$ (diluted gas), the stability criterion (17) agrees with the corresponding results obtained in [12, 17] for the BGK–Vlasov and Boltzmann–Vlasov models, respectively.

J. Stat. Mech. (2019) 103205

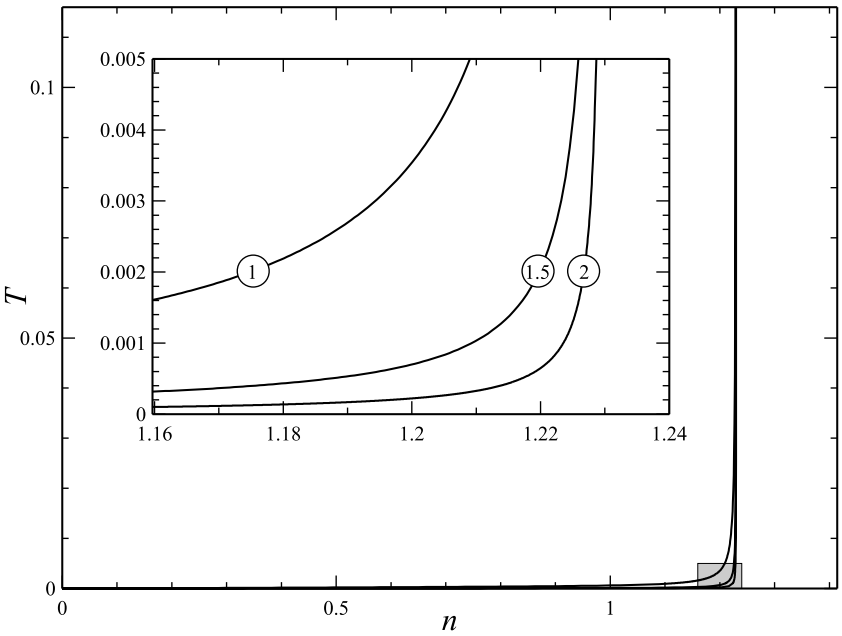

Figure 3. The dependence of the boundary of IR2 on the parameter R of the Fourier transform (22) of the Vlasov potential. The inset shows a blow-up of the shaded region of the main panel. The curves are marked with the corresponding values of R.

5. Discussion

For $k = 0$ (the boundary of IR1), (17) and (19) reduce to

$$T = \frac{n}{1 + \frac{4\pi}{3} n A_1 + \sum_{l=2}^{L} c_l n^l A_l},$$

where constants A_l are given by (11). The above expression can be rewritten in terms of the function $\Theta(n)$ (given by (10)),

$$T = \frac{n}{1 + [n^2 \Theta'(n)]'}. \tag{26}$$

This representation of the boundary of IR1 turns out to be very useful.

(1) Equation (26) implies that IR1 does not depend on the specific shape of the Vlasov potential Φ.

(2) As for IR2, it does depend on Φ, but this dependence is weak—which we illustrate by computing the boundary of IR2 for different values of the parameter R (which appears in expression (22)) and plotting the results in figure 3. One can see that, for $R \gtrsim 2$, the boundary of IR2 is virtually indistinguishable from a vertical line. This effect is even more pronounced if $\hat{\Phi}(k)$ decays exponentially as $k \to \infty$. Given that the van der Waals force is supposed to be long-range (by comparison with the molecule size), one can assume that $R \gg 1$, and thus replace the boundary of IR2 by a vertical line. Physically, this means that a fluid cannot be compressed beyond a certain density value no matter what the temperature is.

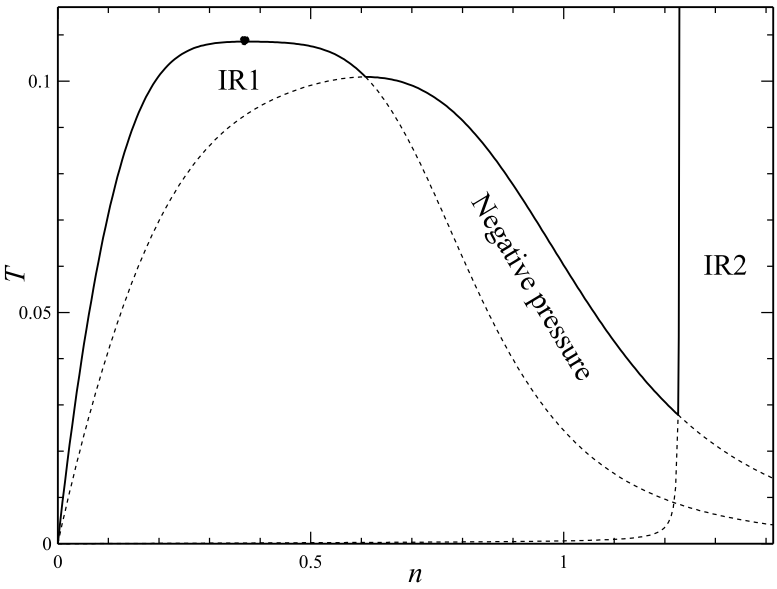

Figure 4. The stable, physically meaningful fluid states in the (n, T) parameter plane. IR1 and IR2 stand for instability regions 1 and 2, respectively. The black dot marks the critical point.

(3) Using EoS (12), one can show that the maximum of the function $T(n)$ given by (26) corresponds to the critical point.

(4) Not all of the stable states are physically meaningful, as some of them correspond to negative pressure. These can be detected using EoS (12). For the case (20)–(22) with $R = 1$, the full diagram of stable and physically meaningful fluid states is shown in figure 4.

(5) As stated in most thermodynamics texts, a non-ideal gas becomes unstable if

$$\left(\frac{\partial p}{\partial n}\right)_{T=\text{const}} < 0, \tag{27}$$

i.e. if an increase of density gives rise to a decrease of pressure. Applying this argument to EoS (12), we recover equation (26) describing the boundary of IR1. IR2, in turn, is located in high-density region—hence, it may only describe fluid-solid transitions. Most importantly, the whole boundary of IR2 corresponds to a single value of the perturbation wavenumber, $k_{1.5}$—so that $2\pi/k_{1.5}$ can be identified with the spatial scale of the emerging crystal. This agrees with the fact that ~~that~~ crystal structure does not depend on the temperature or density of the fluid state where the transition takes place.

(6) It is well-known that gas–liquid transition typically occurs *before* criterion (27) predicts it. The threshold where the actual transition occurs is determined by the so-called evaporation curve describing the gas–liquid equilibrium. It is still possible, however, to overcool a gas or overheat a liquid beyond this threshold, provided they are sufficiently pure. Thus, the boundaries of the instability regions

J. Stat. Mech. (2019) 103205

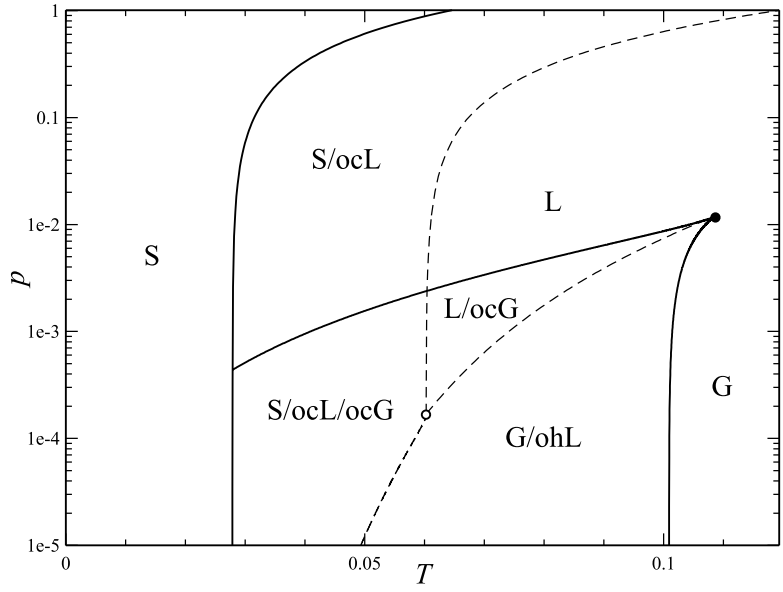

Figure 5. The phase diagram for argon in the nondimensional (T, p) plane. Solid lines correspond to the boundaries of the instability regions computed using the EV model; dashed lines show the empiric evaporation, melting, and sublimation curves [18]. The critical and triple points are marked by a black dot and small circle, respectively. ' G', 'L', and 'S' mark the regions where gas, liquid, and solid may exist; the prefixes 'oc' and 'oh' mean ' overcooled' and 'overheated'.

are essentially the limits to which one can overcool or overheat a fluid before phase transition occurs.

To illustrate this interpretation, we have redrawn figure 4 on the (T, p) plane, thus turning it into a phase diagram—see figure 5. We have also added empirically-derived evaporation, melting, and sublimation curves (the last two describe the solid–liquid and solid–gas equilibria, respectively).

The following features of figure 5 can be observed:

- There are two single-phase regions: in the one marked 'S', only solid phase exists—and in the one whose parts are marked 'L' or 'G', one of the two fluid phases exists (gas and liquid are difficult to separate in the latter case, as they can be continuously transformed one into another).
- In the transitional zone marked 'S/ocL', either solid or overcooled liquid can exist—and in the zone 'S/ocL/ocG', it is either solid or overcooled liquid, or overcooled gas.
- In the remaining two zones, 'L/ocG' and 'G/ohL', either of the two fluid phases can exist.

J. Stat. Mech. (2019) 103205

6. Concluding remarks

In this work, we have used the Enskog–Vlasov model to examine when fluids are unstable, and with respect to which perturbations. The parameter range of the instability is illustrated in figure 4 on the nondimensional (n, T) plane, and in figure 5, on the (T, p) plane. These figures are the main results of this work.

Note that, in figure 5, we have calculated only the solid curves, whereas the dashed ones have been obtained by methods of statistical thermodynamics [18]. This does not mean that the EV model cannot be used to calculate the latter: in fact, it *has* been used for calculating the evaporation curve, producing a result with an error of only several percent [16]. Before calculating the melting and sublimation curves, however, one should explore periodic solutions of the EV equation which describe the solid (crystal) state; these solutions bifurcate from the spatially uniform (fluid) solutions as frozen waves. That is, we do not claim that the EV model can describe the fundamental physics of the solid state—but we do hope that it can 'mimic' it given a suitable choice of the functional $Q[n]$ and the Vlasov potential Φ. In fact, the Enskog approach to dense fluids has been successfully used for describing hard-sphere crystals [19, 20] and studying equilibrium properties of the liquid–solid phase transitions [21, 22] (for recent developments in the latter theory, see [23–26]).

Once the EV model is calibrated to deal with all three phases, it would become an invaluable tool for modeling complex physical problems (e.g. evolution of liquid films with evaporation and solidification). This is an important point, as several version of the Enskog–Vlasov kinetic equation have been used for applications (see [27, 28] and references therein).

Acknowledgments

This work was supported by FCT—Fundação para a Ciência e a Tecnologia of Portugal under Project UID/FIS/50010/2019 and by European Regional Development Fund through the Operational Program of the Autonomous Region of Madeira 2014–2020 under Project PlasMa-M1420-01-0145-FEDER-000016.

References

[1] Enskog D 1922 Kinetische theorie der wärmeleitung, reibung und selbstdiffusion in gewissen verdichteten gasen und flüssigkeiten *Kungl. Sven. Vetenskaps Akad. Handl.* **63** 1–44
[2] de Sobrino L 1967 On the kinetic theory of a van der Waals gas *Can. J. Phys.* **45** 363–85
[3] Lebowitz J L, Percus J K and Sykes J 1969 Kinetic-equation approach to time-dependent correlation functions *Phys. Rev.* **188** 487–504
[4] van Beijeren H and Ernst M H 1973 The modified Enskog equation *Physica* **68** 437–56
[5] Karkheck J and Stell G 1981 Kinetic mean-field theories *J. Chem. Phys.* **75** 1475–87
[6] Stell G, Karkheck J and van Beijeren H 1983 Kinetic mean field theories: results of energy constraint in maximizing entropy *J. Chem. Phys.* **79** 3166–7
[7] Grmela M and Garcia-Colin L S 1980 Compatibility of the Enskog kinetic theory with thermodynamics I *Phys. Rev.* A **22** 1295–304
[8] Benilov E S and Benilov M S 2018 Energy conservation and h theorem for the Enskog–Vlasov equation *Phys. Rev.* E **97** 062115
[9] Grmela M 1971 Kinetic equation approach to phase transitions *J. Stat. Phys.* **3** 347–64

[10] Grmela M and Garcia-Colin L S 1980 Compatibility of the Enskog-like kinetic theory with thermodynamics. II. Chemically reacting fluids *Phys. Rev.* A **22** 1305–14
[11] Grmela M 1981 Entropy principle as a restrictive condition on kinetic equations *Can. J. Phys.* **59** 698–707
[12] Benilov E S and Benilov M S 2016 Semiphenomenological model for gas–liquid phase transitions *Phys. Rev.* E **93** 032148
[13] Fowler A C 2019 Phase transition in the Boltzmann–Vlasov equation *J. Stat. Phys.* **174** 1011–26
[14] Meseguer J, Slobozhanin L A and Perales J M 1995 A review on the stability of liquid bridges *Adv. Space Res.* **16** 5–14
[15] Benilov E S 2016 Stability of a liquid bridge under vibration *Phys. Rev.* E **93** 063118
[16] Benilov E S and Benilov M S 2019 Peculiar property of noble gases and its explanation through the Enskog–Vlasov model *Phys. Rev.* E **99** 012144
[17] Benilov E S and Benilov M S 2017 Kinetic approach to condensation: diatomic gases with dipolar molecules *Phys. Rev.* E **96** 042125
[18] Tegeler C, Span R and Wagner W 1999 A new equation of state for argon covering the fluid region for temperatures from the melting line to 700 K at pressures up to 1000 MPa *J. Phys. Chem. Ref. Data* **28** 779–850
[19] Kirkpatrick T R 1989 Does the velocity autocorrelation function oscillate in a hard-sphere crystal? *J. Stat. Phys.* **57** 483–96
[20] Kirkpatrick T R, Das S P, Ernst M H and Piasecki J 1990 Kinetic theory of transport in a hard sphere crystal *J. Chem. Phys.* **92** 3768–80
[21] Ramakrishnan T V and Yussouff M 1979 First-principles order-parameter theory of freezing *Phys. Rev.* B **19** 2775–94
[22] Haymet A D J and Oxtoby D W 1981 A molecular theory for the solid–liquid interface *J. Chem. Phys.* **74** 2559–65
[23] Archer A J 2009 Dynamical density functional theory for molecular and colloidal fluids: a microscopic approach to fluid mechanics *J. Chem. Phys.* **130** 014509
[24] Lutsko J F 2012 A dynamical theory of nucleation for colloids and macromolecules *J. Chem. Phys.* **136** 034509
[25] Baskaran A, Baskaran A and Lowengrub J 2014 Kinetic density functional theory of freezing *J. Chem. Phys.* **141** 174506
[26] Heinonen V, Achim C V, Kosterlitz J M, Ying S-C, Lowengrub J and Ala-Nissila T 2016 Consistent hydrodynamics for phase field crystals *Phys. Rev. Lett.* **116** 024303
[27] Frezzotti A and Barbante P 2017 Kinetic theory aspects of non-equilibrium liquid–vapor flows *Mech. Eng. Rev.* **4** 16–00540
[28] Frezzotti A, Gibelli L, Lockerby D A and Sprittles J E 2018 Mean-field kinetic theory approach to evaporation of a binary liquid into vacuum *Phys. Rev. Fluids* **3** 054001

J. Stat. Mech. (2019) 103205